Full-length article

CD40L-expressing CD4+ T cells prime adipose-derived stromal cells to produce inflammatory chemokines

Joelle Dulong[1,2,*], Séverine Loisel[1,2,*], Delphine Rossille[1,2], Simon Léonard[1], Nadège Bescher[1,2], Isabelle Bezier[1,2], Maelle Latour[1,2], Céline Monvoisin[1], Delphine Monnier[3], Nicolas Bertheuil[1,2,4], David Roulois[1], Karin Tarte[1,2,3,**]

[1] UMR 1236, Univ Rennes, INSERM, Etablissement Français du Sang Bretagne, Rennes, France
[2] SITI Laboratory, Etablissement Français du Sang Bretagne, CHU Rennes, Rennes, France
[3] Pôle Biologie, CHU Rennes, Rennes, France
[4] Department of Plastic Surgery, CHU Rennes, Rennes, France

ARTICLE INFO

ABSTRACT

The therapeutic potential of culture-adapted adipose-derived stromal cells (ASCs) is largely related to their production of immunosuppressive factors that are inducible *in vitro* by priming with inflammatory stimuli, in particular tumor necrosis factor-α (TNFα) and interferon-γ (IFNγ). *In vivo*, obesity is associated with chronic inflammation of white adipose tissue, including accumulation of neutrophils, infiltration by IFNγ/TNFα-producing immune cells, and ASC dysfunction. In the current study, we identified in obese patients a simultaneous upregulation of *CD40L* in the adipose tissue stroma vascular fraction (AT-SVF), correlated with the Th1 gene signature, and an overexpression of CD40 by native ASCs. Moreover, activated CD4+ T cells upregulated CD40 on culture-expanded ASCs and triggered their production of IL-8 in a CD40L-dependent manner, leading to an increased capacity to recruit neutrophils. Finally, activation of ASCs by sCD40L or CD40L-expressing CD4+ T cells relies on both canonical and non-canonical NF-κB pathways, and *IL-8* was found to be coregulated with NF-κB family members in AT-SVF. These data identify the CD40-CD40L axis as a priming mechanism of ASCs, able to modulate their cross talk with neutrophils in an inflammatory context, and their functional capacity for therapeutic applications.

Introduction

White adipose tissue (WAT) contains large amounts of adipose progenitor cells considered a valuable source of clinical-grade stromal cells after *in vitro* expansion. Culture-adapted adipose-derived stromal cells (ASCs) are a promising therapeutic alternative in a broad range of clinical applications, including inflammatory diseases and chronic degenerative disorders, owing to their anti-inflammatory and immunosuppressive properties [1]. In fact, *in vitro*−expanded ASCs and bone marrow−derived mesenchymal stromal cells (BM-MSCs), despite sharing inhibitory activity toward all components of innate and adaptive immunity, display distinctive phenotypic, transcriptomic, and functional features, and ASCs have recently emerged as easier to harvest, more immunosuppressive, and less immunogenic than BM-MSCs [2−4]. Such specificities are shared by their native counterparts, highlighting an imprinting of tissue source on cultured MSC immune properties [2]. Yet the main driver of MSC immune functions is their response to inflammatory stimuli, with tumor necrosis factor-α (TNFα) and interferon-γ (IFNγ) acknowledged as key inducers of the complex pattern of MSC immunosuppressive determinants *in vitro* [5,6]. How such factors, produced by activated immune cells, impact the immune properties of MSCs *in vivo* remains largely underexplored.

Obesity is characterized by chronic inflammation of WAT, associated with remodeling of immune cell landscape, including recruitment of proinflammatory and profibrotic macrophages together with type 1 immune cells such as CD8+ T cells, IFNγ-producing T helper 1 (Th1) CD4+ T cells, or natural killer (NK) cells [7,8,9]. Their role in obesity is less well studied, but neutrophils accumulate early upon high-fat diet feeding in mice [10] and are the most important fat myeloid subset in morbidly obese patients, strongly decreasing after losing weight [11]. In obesity, adipocytes themselves are dysfunctional and display proinflammatory properties [12]. Furthermore, ASCs expanded from obese patients exhibit an altered transcriptomic profile, with upregulation of adipogenic and inflammatory genes,

** Corresponding author: Karin Tarte, INSERM U1236, Faculté de Médecine, 2 Avenue du Pr Léon Bernard, 35043 RENNES, France. Phone: +33 2 23 23 45 12, fax: +33 2 23 23 49 58.

E-mail address: karin.tarte@univ-rennes1.fr (K. Tarte).

* J. Dulong and S. Loisel contributed equally to this work.

including CXCL8/IL8 and CCL2 chemokines [13]. Moreover, they display superior migratory but weaker immunosuppressive capacities compared with ASCs expanded from lean donors, and interleukin (IL)-1β was proposed as partly involved in obesity-related ASC immune dysfunctions [14,15,16]. However, the mechanisms involved in the interplay between native and culture-adapted ASCs and immune cells are poorly described.

The CD40-CD40 ligand (CD40L) pathway is involved in WAT inflammation during obesity [17]. CD40L is produced by activated CD4$^+$ T cells, and its circulating soluble form (sCD40L) is increased in obese patients and correlated to body mass index (BMI) [18,19]. Moreover, mature adipocytes express CD40 and respond to CD40L activation by upregulating IL-6, CCL2, and TNFα proinflammatory factors [20]. Whereas CD40 is detectable on the surface of native BM-MSCs [21] and is upregulated by inflammatory stimuli on culture-adapted BM-MSCs and ASCs [4], no study has explored whether CD40 is expressed on native ASCs and could directly affect their immune functions.

In the current work, we studied CD40-CD40L axis deregulation in adipose tissue from obese *versus* lean patients and evaluated the mechanisms and consequences of CD4$^+$ T cell−derived CD40L stimulation in ASCs, with a particular interest in its impact on the cross talk between ASCs and neutrophils.

Material and Methods

ASCs and immune cell production

Donor recruitment followed institutional review board approval, and written informed consent process according to the revised Declaration of Helsinki was obtained. Adipose tissue stromal vascular fractions (AT-SVFs) were obtained from obese (BMI, 39.6 [35.5, 46], median [minimum, maximum]) and lean (24.4 [21.7, 25]) WAT donors (**Supplementary Table S1**). Lipoaspirates were harvested at the beginning of abdominoplasty using the traditional suction-assisted lipectomy and were then digested with 200 IU/mL CLS4 collagenase (Worthington), 1.6 IU/mL NPRO dispase (Worthington), and 10 IU/mL DNAse (Pulmozyme; Roche) for 45 min at 37°C, filtrated, and centrifuged, and the resulting AT-SVFs were frozen. Thawed AT-SVFs were then used for sorting DAPI$^-$CD45$^-$CD11b$^-$CD235a$^-$CD31$^-$CD146$^-$CD34$^+$ viable native ASCs using a FACSAria II (BD Biosciences) as previously described [2] or seeded at 1,000 cells/cm^2 in αMEM (Invitrogen) supplemented with 10% fetal calf serum (FCS; Biosera), 100 IU/mL penicillin, 100 μg/mL streptomycin (Invitrogen), and 1 ng/mL fibroblast growth factor β (Cellgenix). Culture medium was renewed every 3 to 4 days until the cells reached near-confluence (end of passage 0 [P0]). ASCs were then detached using trypsin and used at P1 for phenotypic and functional experiments. The lack of hematopoietic and endothelial cells within DAPI$^-$ viable cells was validated by flow cytometry using phycoerythrin (PE)-conjugated anti-CD90, BUV395-conjugated anti-CD45, BV786-conjugated anti-CD31 (all from BD), and APC-conjugated anti-CD73 (Miltenyi Biotech) monoclonal antibodies (mAbs) and their isotypic controls (**Supplementary Figure S1**).

CD4$^+$ T cells and monocytes were isolated from peripheral blood mononuclear cells (PBMCs) and polynuclear neutrophils from blood samples using a CD4$^+$ T cell isolation kit, a pan monocyte isolation kit, and whole blood CD15 MicroBeads (Miltenyi Biotec), respectively.

Gene expression profiling of AT-SVF

RNA was extracted from AT-SVF using the Nucleospin RNA XS Micro kit (Macherey Nagel), and gene expression level was assessed using the Fluidigm BioMark HD system. Briefly, cDNAs were obtained using the Fluidigm reverse transcription Master Mix and preamplified for 14 cycles in the presence of Pre-Amp Master Mix and pooled Taqman assay mix (**Supplementary Table S2**). Gene expression was then measured with the TaqMan Gene Expression Master Mix (Thermo Fisher) on a 48.48 Dynamic Array IFC. After a quality control check, gene expression was calculated with the ΔCT calculation method and *CDKN1B, EIF2B1*, and *PUM1* as housekeeping genes. Principal component analysis (PCA) was done on the 41 expressed genes with the prcomp() R function and visualized using the Factoextra R package (version 1.0.7). Eigengene values of the first dimension of PCA (DIM1) were then visualized through a dot plot. We used the function fviz_contrib() to identify the genes that contributed more than average to the DIM1 axis. Levels of expression of these 23 genes were then visualized via heatmap with the package pheatmap (version 1.0.12).

ASC activation

For T cell activation, purified CD4$^+$ T cells were cultured in RPMI and 10% human AB serum (Eurobio), 10 IU/mL recombinant human IL2 (rhIL2, Proleukin; Clinigen), and 5 μg/mL concanavalin A (Sigma-Aldrich). On day 3, 20 IU/mL rhIL2 was added, and on day 7, T cells were restimulated with 0.1 μM phorbol 12-myristate 13-acetate and 10 μM ionomycin (Sigma-Aldrich) for the last 5 hours. CD40L protein membrane expression was then checked by flow cytometry using PE-conjugated anti-CD40L mAb (Beckman Coulter) or appropriate isotype control.

Confluent monolayers of P1 ASCs were treated or not with 100 IU/mL IFNγ, 50 ng/mL TNFα (Bio-techne), soluble CD40L (Immunex, 1.5 μg/ml for evaluation of nuclear factor-κB (NF-κB) pathway activation or 300 ng/ml for functional experiments) or activated third-party CD4$^+$ T cells (1:45, T/ASC ratio) for the indicated times. Supernatant was frozen, and ASCs were collected for flow cytometry and RNA extraction. In co-culture experiments with activated CD4$^+$ T cells, ASCs were sorted as CD45$^-$CD105$^+$ cells using fluorescein isothiocyanate (FITC)-conjugated anti-human CD45 (Beckman Coulter) and PE-conjugated anti-human CD105 (Beckman Coulter) mAbs before RNA extraction. In some experiments, ASCs were transfected before stimulation with control, *CD40* (three different small interfering RNAs [siRNAs], 50 nM each), *RELA* (three different siRNAs, 5 nM each), or *NFKB2* (three different siRNAs, 50 nM each) siRNA (Life Technologie) using HiPerfect (Qiagen) following manufacturer instructions. Efficacy of siRNA was evaluated by quantitative polymerase chain reaction (QPCR) for corresponding genes (**Supplementary Figure S2**).

Evaluation of CD40 and chemokine expression in ASCs

After *ex vivo*−expanded ASC activation, CD40 surface expression was evaluated by flow cytometry on CD45$^-$CD105$^+$ cells using PE-conjugated anti-CD40 mAb (Diaclone) and appropriate isotype control and analysis on a Fortessa X20 (BD). Moreover, *CCL2, CCL5, IL8, CD40,* and *IL6* were quantified by reverse-transcription (RT)-QPCR. Briefly, cDNA synthesis was performed with the Superscript II reverse-transcriptase (Invitrogen) and assay-on-demand primers and probes, and Taqman Universal MasterMix was used to run QPCR on a StepOnePlus Real Time PCR System (Applied Biosystems). PCR data were normalized to the geometric mean of three housekeeping genes (*PUM1, CDKN1B,* and *EIF2B1*). Results were further standardized by comparison to gene expression of a pool of five MSCs when mentioned. Similarly, *CD40* expression was quantified by RT-QPCR on sorted native ASCs using the same housekeeping genes.

CCL2, CCL5, and IL8 protein levels were also quantified in ASC supernatants by ELISA (Bio-Techne) according to the manufacturer instructions. The minimum value was the detection threshold of the method.

NFκB pathway activation study

NF-κB pathway activation was evaluated using the Nuclear Extract kit and the TransAM NFκB Family Kits (Active Motif) according to manufacturer instructions using a Varioskan (Thermo Fisher) to read absorbance. NF-κB1 and RELA activation were evaluated after 1 hour of stimulation, and NF-κB2 and RELB after 5 hours of stimulation, by 1.5 μg/mL CD40L.

RELA nuclear translocation was evaluated by immunofluorescence on a SP5 microscope (Leica) after 30 min of stimulation by 1.5 μg/mL CD40L. After 15 min of methanol fixation at −20°C, cells were incubated with PBS bovine serum albumin (BSA; Sigma Aldrich) for 1 hour at 37°C, before adding anti-RELA antibody (1/400; Cell Signaling) overnight at 4°C and secondary antibody goat anti-rabbit IgG (Invitrogen) for 1 hour at room temperature. After washing, cells were mounted with Moviol containing sytox blue (Thermo Fisher) for nuclear labeling. The colocalization between nucleus and RELA staining was evaluated using the plugin Colocalization Threshold in Fiji software.

Neutrophil and monocyte migration

After 3 days of ASC stimulation (300 ng/mL sCD40L or co-culture with activated CD4+ T cells), the medium was replaced by a migration medium (RPMI and 0.1% human serum albumin (Vialebex; LFB) for neutrophils and RPMI and 1% FCS for monocytes [22]) for 3 days before supernatant collection.

Neutrophils and monocytes were added at 10^5 cells/100 μL in migration medium to the upper compartment of Transwell chambers with 5-μm pore filters (Corning Costar); lower chambers contained ASC-conditioned migration medium. Supernatants from ASC/T cell co-culture experiments were diluted 1:3 before their use in migration assays. When indicated, 10 μg/mL anti-CXCR1 blocking antibody or isotype control (Bio-Techne) was added in the lower chamber. The absolute number of viable DAPI−CD45+ neutrophils or DAPI−CD14+ monocytes in the lower chamber was quantified with FlowCount beads (Beckman Coulter). The percentage of cell migration was determined by comparing the number of viable cells in the lower compartment after 2 hours of migration with the initial number of cells seeded in the upper compartment.

Neutrophil survival

After 3 days of ASC stimulation (300 ng/mL sCD40L), purified neutrophils were co-cultured with or without ASCs (neutrophil/ASC ratio 2.5:1). The absolute number of viable DAPI−CD45+ neutrophils was evaluated by flow cytometry with FlowCount beads after 2 days of culture.

Statistical analysis

Statistical analyses were performed with Prism software version 9.1.2 (GraphPad Software) and R version 3.6.0 (www.R_project.org). The Wilcoxon test was used for matched pairs, and the Mann−Whitney *U* test for nonpaired samples. When indicated, the normality of distribution was tested by a Shapiro−Wilk test before using paired *t* test. The fold-change is the ratio of median values.

The co-expression of *NFKB1, NFKB2, RELA, RELB,* and *CXCL8* as well as the correlation between *TBX21, CD40LG,* and *IFNG* were evaluated by Pearson correlation analysis between two variables and visualized on a matrix with package R corrplot version 0.84.

Results

Inflammation induces CD40 on ASCs

To explore the inflammatory context in obese patients, we analyzed by QPCR the expression of 44 inflammation-related genes in AT-SVF obtained from 10 obese and nine lean patients. Gene expression profile of the 41 detectable genes was analyzed in a nonsupervised manner through PCA (**Figure 1**A). Interestingly, AT-SVF samples coming from obese *versus* lean patients were differentially organized along the first dimension of the PCA (DIM1, $P<$ 0.05) (**Figure 1**B). The 23 genes contributing more than average to PCA DIM1 (**Supplementary Figure S3A**) identified a pattern of genes overexpressed in obese patients (**Figure 1**C) and essentially included T cell and myeloid cell markers. *CCL2, CCL5,* and *CXCL8,* three inflammatory chemokines involved in the recruitment of myeloid cells, belonged to this 23-gene panel together with the *CD68* and *CSF1R* macrophage markers. In agreement, *ADIPOQ,* the gene coding for the anti-inflammatory factor adiponectin known to suppress M1 macrophage activation [23], was significantly reduced in obese patients (**Supplementary Figure S3B**). Moreover, both *TBX21* and *GATA3,* the drivers of Th1 versus Th2 T cell differentiation, were found to be differentially expressed between obese and lean patients ($P < 0.05$), and *TBX21* expression was found to be strongly correlated with *IFNG* and *CD40LG* ($P=$ 0.002 and $P = 2.97 \times 10^{-5}$, respectively; **Figure 1**D), suggesting an enrichment for functional Th1 cells in obese patients and highlighting for the first time an overexpression of *CD40LG* in obese AT-SVFs (P < 0.01, Figure 1E). We thus evaluated *CD40* expression by purified ASCs and revealed its overexpression in a series of obese (n = 5) versus lean (n = 5) native ASCs ($P < 0.01$) (Figure 1F). Interestingly, analysis of public single-cell RNA-sequencing data obtained from frozen WAT [24] identified native ASCs (corresponding to preadipocyte and adipose precursor cell clusters) as the main CD40-expressing cells within AT-SVF (Supplementary Figure S4A, B). These data suggest that the CD40-CD40L pathway could be active in WAT from obese patients and does not involve only mature adipocytes but also CD40-expressing ASCs.

To better understand the signals triggered by CD40 upregulation on ASCs, we stimulated short-term-expanded ASCs by various inflammatory stimuli produced by activated Th1 cells, including sCD40L, TNFα, and IFNγ, or by CD4+ T cells activated *in vitro* to express CD40L (**Supplementary Figure S4C**). Whereas sCD40L did not increase CD40-, IFNγ-, or TNFα-induced CD40 overexpression on ASCs as single agents, at either the mRNA or protein level (**Figure 1 G, H and Supplementary Figure S4D, E**), *CD40* induction similar to that obtained in ASC co-culture with activated CD4+ T cells was reached when combining IFNγ, TNFα, and sCD40L, with a ∼65-fold increase of *CD40* expression compared with resting ASCs. Overall, we confirmed that inflammatory cytokines, but also direct contact with activated CD4+ T cells, upregulates CD40 expression on *in vitro*−expanded ASCs, as in ASCs from obese patients.

CD40L triggers inflammatory chemokine overexpression in ASCs

After the demonstration of CD40 induction on ASCs exposed to inflammatory stimuli *in vitro* and *in vivo*, we decided to investigate the impact of CD40 activation on ASC properties, with a particular interest in their production of chemokines, a key step in MSC immunosuppressive properties [25]. Stimulation of *in vitro*−expanded ASCs by sCD40L upregulated their expression of CCL2, CCL5, and IL-8 at the mRNA and protein levels (**Figure 2 A, B**). Given the huge infiltration of WAT from obese patients by neutrophils [11], we further explored IL-8 production by primed ASCs. Activated CD4+ T cells strongly increased IL-8 production by ASCs, and this induction was significantly reduced by decreasing ASC CD40 expression by a CD40 siRNA (**Figure 2**C), demonstrating a role for the CD40L-CD40 pathway in T cell−dependent ASC activation. We next explored the ability of the IL-8 produced by ASCs to recruit neutrophils. For that purpose, we quantified by flow cytometry the number of neutrophils migrating toward supernatants from unstimulated and sCD40L-stimulated ASCs through Transwell chambers (**Figure 2**D). Interestingly, sCD40L-stimulated ASCs were more potent to recruit neutrophils
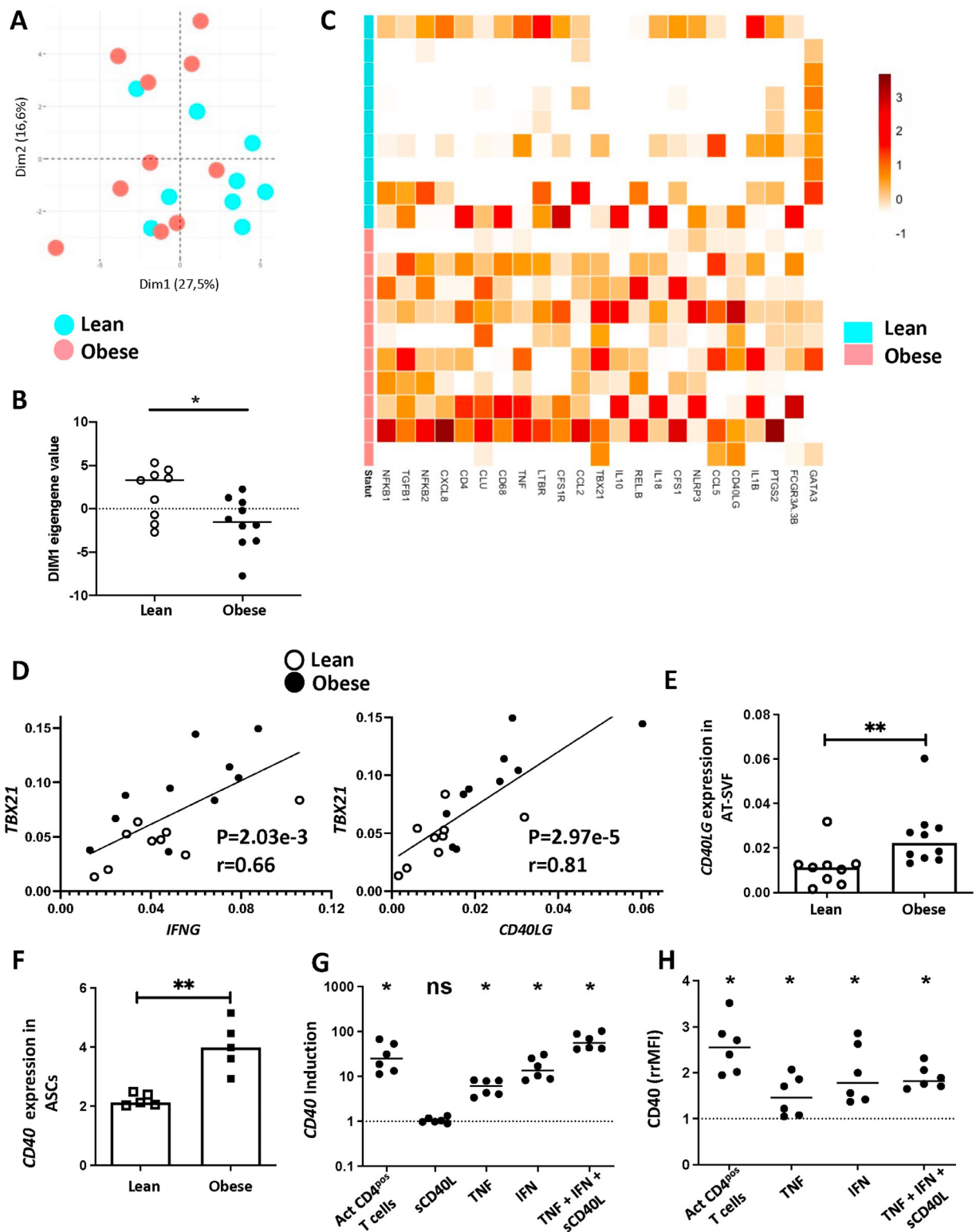
Figure 1. Inflammatory context induces CD40 on ASC in vitro and in vivo. **(A−E)** AT-SVFs from obese (n = 10) and lean (n = 9) donors were studied by RT-QPCR for a panel of inflammation-related genes. (A) Unsupervised analysis of the gene expression profile of the 41 expressed genes by PCA. (B) Scatterplot visualization of the first dimension of the PCA (DIM1) eigengene value of each AT-SVF sample; *P < 0.05. (C) Heatmap representation of the 23 genes contributing more than average to PCA DIM1. (D) Correlation between *TBX21* and *IFNG* and between *TBX21* and *CD40LG* across the 19 AT-SVF samples. (E) Expression of *CD40LG*; **P < 0.01. (F) DAPI−CD45−CD11b−CD235a−CD31−CD146−CD34+ viable native ASCs were sorted from obese (n = 10) and lean (n = 9) obese patients and studied for CD40 expression by RT-QPCR; **P < 0.01. (G and H) *In vitro*−expanded ASCs were activated by sCD40L, TNFα (TNF), IFNγ (IFN), or an activation cocktail containing TNF, IFN, and sCD40L. ASCs were also stimulated by activated CD40L-expressing CD4+ T cells (Act CD4+ T cells) before sorting (for RNA extraction) or gating (for flow cytometry experiments) of CD45−CD105+ primed ASCs. (G) *CD40* mRNA expression was measured by RT-QPCR after 24 hours of ASC activation (n = 6 ASC batches), normalized to three housekeeping genes, and represented in arbitrary units obtained by assigning the value of 1 to nonstimulated ASCs (dotted lines). (H) CD40 protein membrane expression was also quantified by flow cytometry after 2 days (n = 6 ASC batches). The ratio of CD40 mean fluorescence intensity (MFI) to isotype control MFI (rMFI) was normalized to 1 for the rMFI obtained with nonstimulated ASCs (dotted line), and the relative rMFIs (rrMFI) of CD40 between stimulated and nonstimulated ASCs are represented. Bars: medians from independent experiments. *P < 0.05; ns, not significant.
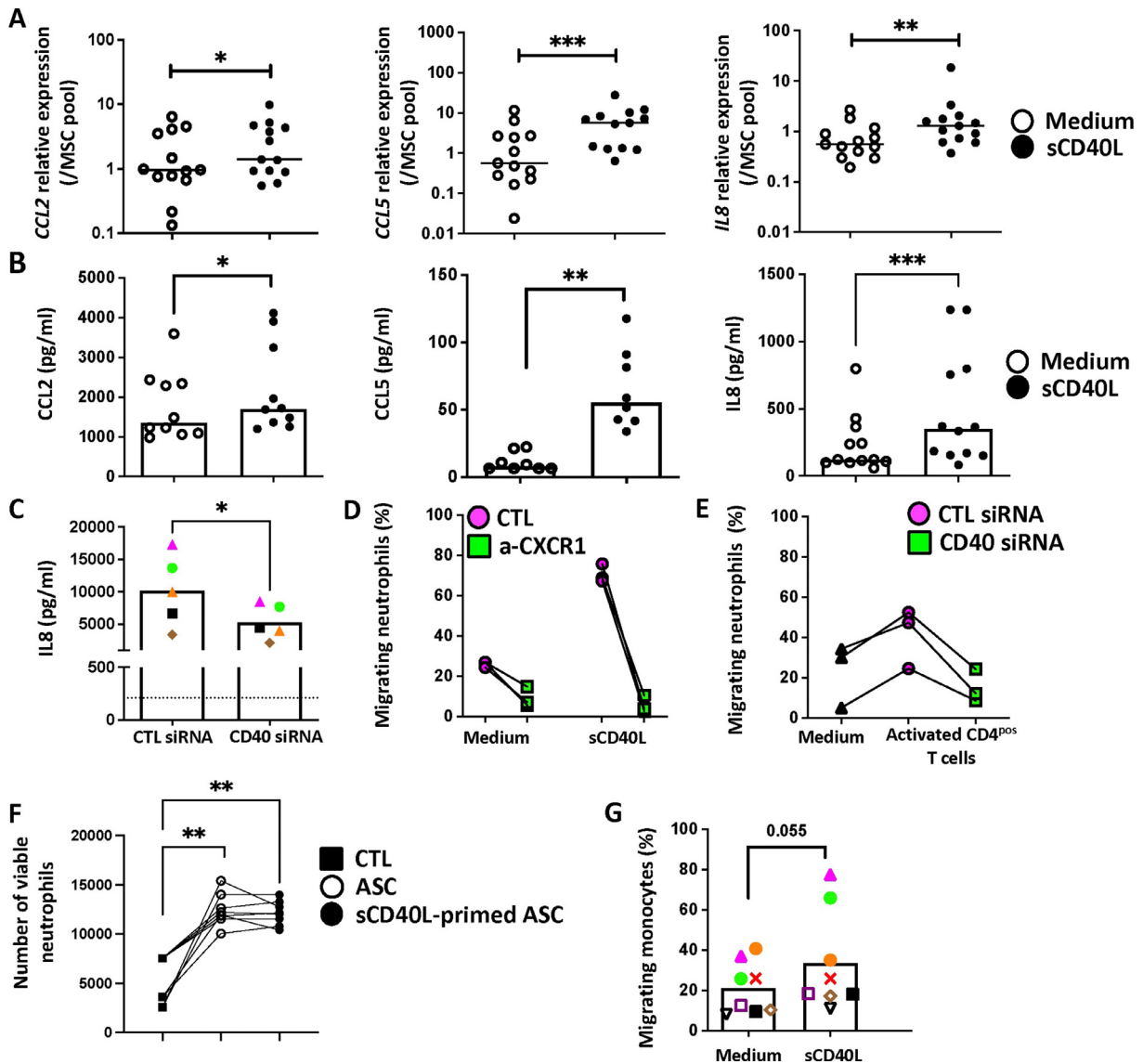
Figure 2. CD40L triggers chemokine overexpression and neutrophil recruitment by ASCs. (A and B) ASCs were cultured with (black symbols) or without (open symbols) sCD40L. (A) *CCL2, CCL5,* and *IL-8* were quantified by RT-QPCR after 24 hours of culture (n = 13 ASC batches), normalized to three housekeeping genes, and represented in arbitrary units obtained by assigning the value of 1 to a pool of MSCs. (B) CCL2, CCL5, and IL-8 protein levels were quantified in cell supernatant by ELISA after 3 days of culture (n = 10, n = 8, n = 12 ASC batches; respectively). (C) ASCs were transfected with control (CTL) or CD40 siRNA (three different siRNAs; 50 nM each) before co-culture with activated CD4$^+$ T cells (n = 5 ASC batches). IL-8 protein level was quantified in the supernatant by ELISA after 3 days of culture. Dotted line represents the average of IL-8 levels found in the supernatant of ASCs cultured without activated CD4$^+$ T cells. Each symbol corresponds to an individual experiment. Statistical analysis was performed using paired *t* test after testing the normality of the distribution. (D) ASCs were cultured for 3 days with or without (medium) sCD40L before medium replacement. Supernatants were then collected and tested for their capacity to trigger neutrophil recruitment in 2 hours through a 5-μM Transwell. Anti-CXCR1 blocking monoclonal antibody (a-CXCR1; 10 μg/mL, green square) or its isotype control (CTL, 10 μg/mL, pink circle) was added in the lower chamber. (E) ASCs were cultured for 3 days with or without (medium) activated CD4$^+$ T cells before medium replacement. Supernatants were then collected and tested for their capacity to trigger neutrophil recruitment through a 5-μM Transwell. When indicated, ASCs were transfected with control (CTL siRNA, pink circle) or CD40 (CD40 siRNA, green square) siRNAs before co-culture. (F) ASCs were cultured for 3 days with or without (medium) sCD40L before co-culture with neutrophils (neutrophil/ASC ratio, 2.5:1) for 2 days. The number of viable neutrophils was determined by flow cytometry. Shown are the data obtained using eight ASC batches and neutrophils purified from three donors. (G) ASCs were cultured for 3 days with or without (medium) soluble CD40L (sCD40L) before medium replacement. Supernatants were then collected and tested for their capacity to trigger monocyte recruitment through a 5-μM Transwell. Each symbol corresponds to an individual experiment (n = 8 ASC batches). Statistical analysis was performed using Wilcoxon matched-pairs test.

than unstimulated ASCs, and neutrophil migration was completely abrogated by blocking the IL-8 receptor CXCR1 by an antagonist antibody, demonstrating that neutrophil recruitment by resting and CD40L-primed ASCs was dependent on IL-8. To further investigate the relevance of these data, we next assessed whether supernatants from ASC co-cultured with activated CD4$^+$ T cells were able to trigger the same effect on neutrophil migration (**Figure 2E**). Of note, diluted supernatant (1:3) from T cell−primed ASCs were used to obtain the maximum neutrophil migration (data not shown). Neutrophil migration was higher in response to CD4$^+$ T cell−stimulated ASCs than

resting ASCs and was suppressed when ASCs had been transduced by CD40 siRNA before co-culture with T cells, indicating that CD4$^+$ T cells increased the capacity of ASCs to recruit neutrophils through CD40-CD40L−dependent IL-8 induction. BM-MSCs are well known to protect neutrophils from apoptosis [22,26], and we thus evaluated whether ASCs displayed the same properties and how the process could be affected by CD40 stimulation. Interestingly, resting and sCD40L-primed ASCs strongly and similarly decreased neutrophil spontaneous cell death *in vitro* (**Figure 2F**). Of note, despite the slight upregulation of CCL2 production in sCD40L-activated ASCs

(**Figure 2A, B**), the resulting increase of monocyte migration remained nonsignificant (**Figure 2G**), highlighting neutrophils as a major target of CD40 signaling in ASCs.

NF-κB mediates ASC activation by T cell−derived CD40L

CD40 activity has never been studied on ASCs, and we decided to explore the molecular mechanisms underlying its activation by CD40L. Because both canonical (*NFKB1*) and non-canonical (*RELB, NFKB2*) genes participated in the 23-gene pattern overexpressed in obese AT-SVF (**Figure 1C**), and given the well-known activation of both NF-κB pathways in immune cells by CD40L [27], we evaluated the activation of NF-κB by sCD40L in ASCs. Enzyme-linked immunosorbent assay (ELISA)-based transcription factor activation assays highlighted activation of both canonical and non-canonical NF-κB pathways in ASCs after exposure to sCD40L (**Figure 3A**). Moreover, we confirmed by confocal microscopy the translocation of the NF-κB subunit RelA to the nucleus after CD40 engagement on ASCs (**Figure 3B**). We then assessed whether activation of canonical and non-canonical NF-κB pathways contributed to IL-8 production triggered by sCD40L and activated CD4+ T cells in ASCs using validated (**Supplementary Figure S2**) siRNAs targeting *RELA* and *NFKB2*. Interestingly, IL-8 production was significantly decreased by these two siRNA, independently of the source of CD40L (sCD40L or activated CD4+ T cells) (**Figure 3C**), leading to a decrease of neutrophil recruitment (**Figure 3D**). Finally, *IL-8* was found to be coregulated with NF-κB family members in WAT, as highlighted by a Pearson correlation performed on our series of 19 AT-SVF (**Supplementary Figure S5**),

supporting a role for NF-κB in IL-8 expression in adipose tissue. Overall, these data support the hypothesis that CD4+ T cells induce IL-8 production and neutrophil recruitment by ASCs through the activation of both canonical and non-canonical NF-κB pathways by CD40-CD40L interaction, therefore participating in the inflammatory context seen in AT-SVFs from obese patients.

Discussion

Accumulated evidence suggests that MSC immunosuppressive activity is essentially inducible by inflammatory stimuli but, besides well-described TNFα, IFNγ, and Toll-like receptor (TLR) ligands, few data are available about the impact of other immune cell−derived factors on MSC immunoregulatory functions. In the current study, we identified the CD40L-CD40 axis as a new pathway involved in T cell/MSC cross talk and demonstrated that it could modulate the capacity of native and culture-adapted ASCs to interact with neutrophils.

Mature adipocytes have been shown to express CD40 [20], similarly to BM-MSCs that display increased CD40 expression in response to *in vitro* inflammatory stimuli [28]. We report here that ASCs also express CD40, in particular within inflamed WAT of obese patients and under stimulation by activated CD4+ T cell signaling *in vitro*. A role for the CD40-CD40L axis in the interplay between stromal cells and CD4+ T cells has been reported for murine fibroblastic reticular cells (FRCs), the specialized lymph node stromal cells regulating immune response initiation, maintenance, and control. In this context, activated T cells increase production of inflammatory chemokines, including CCL5, by FRCs, in a CD40L-dependent manner [29].
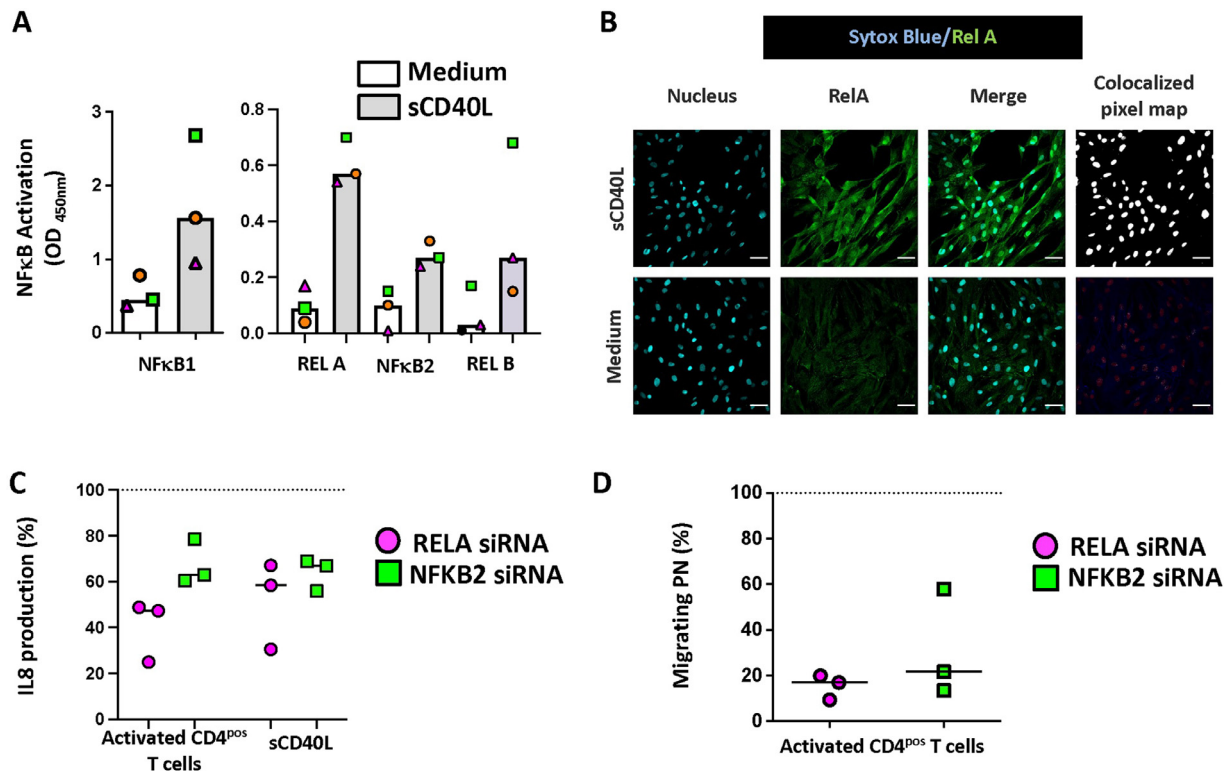

Figure 3. CD40 functional signaling in ASCs is mediated through the NF-kB pathway. (A) ASCs were treated with (gray bars) or without (medium, open bars) sCD40L. NF-κB activation was evaluated after 1 hour (NF-κB1 and RELA) or 5 hours (NF-κB2 and RELB) of culture by an ELISA specific for activated DNA-binding forms of each NF-κB factor (n = 3 ASC batches). (B) ASCs were cultured on glass cover slides and treated with or without (medium) sCD40L. RELA nuclear translocation was evaluated by immunofluorescence after 30 min of stimulation with anti-RELA antibody (green) and nucleus labeling (Sytox blue, blue). The scale bar represents 100 μm; the blank dots represent colocalization. Shown is one representative experiment of three. (C) ASCs were transfected with control, RELA (pink circle), or NF-κB2 (green square) siRNAs before culture with activated CD4+ T cells (n = 3 ASC batches) or sCD40L (n = 3 ASC batches). IL-8 levels were quantified in the supernatant by ELISA after 2 days (sCD40L) or 3 days (activated CD4+ T cells) of culture and normalized to 100% for the IL-8 quantification obtained with control siRNA-transfected ASCs (dotted lines). (D) ASCs were transfected with control, RELA (pink circle), or NF-κB2 (green square) siRNAs before culture with activated CD4+ T cells (n = 3 ASC batches). Supernatants were then collected and tested for their capacity to trigger neutrophil recruitment in 2 hours through a 5-μM Transwell. The percentage of migrating neutrophils was normalized to 100% for the migration measured with supernatants from control siRNA-transfected ASCs (dotted lines).

Interestingly, BM-MSC activation by CD40L-expressing mast cells contributes to disease progression in splenic marginal zone lymphoma [30], and mast cells accumulate in WAT from obese patients [8], suggesting they could participate in CD40-dependent activation of ASCs. Of note, activated neutrophils could express CD40L [31] and CD40 [32], making them able to directly interact with both CD40-expressing ASCs and CD40L-expressing CD4$^+$ T cells, thus reinforcing this ASC−T cell−neutrophil activation loop.

MSC immune functions involve early interaction with neutrophils. BM-MSCs recruit neutrophils, in particular after priming by inflammatory stimuli, and sustain their survival through IL-6 production [26]. Interestingly, CD40 activation did not upregulate *IL-6* in ASCs (**Supplementary Figure S6**), in agreement with their similar capacity to inhibit neutrophil apoptosis *in vitro* compared with resting ASCs. BM-MSCs also downregulate oxidative burst through ICAM1-dependent neutrophil engulfment and extracellular release of the antioxidant superoxide dismutase 3, while inhibiting the formation of neutrophil extracellular trap (NET) and preventing neutrophil-related tissue damage [33,34]. Similarly, amniotic membrane MSCs decrease NET release as well as the production of reactive oxygen species through producing TNFα-stimulated gene 6 protein (TSG-6) [35]. Few data are available on the inhibition of neutrophil activity by ASCs, but their clinical efficacy in cornea repair was attributed to their capacity to trigger neutrophil clearance in a preclinical mouse model [36]. In our study, the use of frozen AT-SVFs precluded any analysis of neutrophil infiltration and activation *in situ*. How ASC inhibitory functions toward neutrophils could reduce inflammatory responses in obese patients thus remains to be explored. Of note, IL-1β was recently shown to collaborate with TNFα/IFNγ to upregulate IL-8 production and resulting neutrophil migration in BM-MSCs in a NF-κB−dependent manner [37]. These data suggest that other NF-κB−activating stimuli could synergize with CD40L in triggering neutrophil recruitment by primed MSCs. IFNγ is produced by CD40L-expressing Th1 cells and is overexpressed in obese WAT, whereas TNFα upregulates IFN-γR [37] and CD40 (our study) on MSCs, underlying the capacity of MSCs to respond to complex inflammatory molecular patterns.

Culture-adapted ASCs are intrinsically more efficient than BM-MSCs at recruiting neutrophils and overexpress TSG-6, involved in the early inhibition of neutrophil and macrophage activity, a specific feature imprinted by their tissue origin [2]. ASCs also overexpress NF-κB family members compared with their BM counterparts and are considered to be FRC precursors [38]. It is thus tempting to speculate that expression of functional CD40 should thus be taken into account when generating ASCs for clinical application, in particular considering the huge amount of sCD40L present in platelet lysate-containing medium frequently used to produce clinical-grade ASCs [39]. Given the major role of MSC−neutrophil interaction in MSC immunosuppressive activity, and the increasing interest in ASCs in MSC-based clinical trials at the expense of their BM counterparts, our work could pave the way for an integration of CD40-CD40L as an MSC priming pathway with physiopathological and clinical impact.

Conflict-of-interest Disclosure

Authors have no competing interests to declare.

Author Contributions

JD, SLo: designed and performed experiments, analyzed data, and contributed writing; DRos, SLe: performed statistical analyzes; NBes, IB, ML, CM: provided technical assistance; DM: contributed to the study design; NBer: provided adipose tissue; DRou: analyzed data and contributed writing; KT: designed and supervised research, analyzed data, and wrote the paper.

All authors have approved the final manuscript.

Supplementary materials

Supplementary material associated with this article can be found in the online version at doi:10.1016/j.jcyt.2022.01.006.

References

[1] Shi Y, Wang Y, Li Q, Liu K, Hou J, Shao C, et al. Immunoregulatory mechanisms of mesenchymal stem and stromal cells in inflammatory diseases. Nat Rev Nephrol 2018;14:493−507. https://doi.org/10.1038/s41581-018-0023-5.

[2] Ménard C, Dulong J, Roulois D, Hébraud B, Verdière L, Pangault C, et al. Integrated transcriptomic, phenotypic, and functional study reveals tissue-specific immune properties of mesenchymal stromal cells. Stem Cells 2020;38:146−59. https://doi.org/10.1002/stem.3077.

[3] Melief SM, Zwaginga JJ, Fibbe WE, Roelofs H. Adipose tissue-derived multipotent stromal cells have a higher immunomodulatory capacity than their bone marrow-derived counterparts. Stem Cells Transl Med 2013;2:455−63. https://doi.org/10.5966/sctm.2012-0184.

[4] Menard C, Pacelli L, Bassi G, Dulong J, Bifari F, Bezier I, et al. Clinical-Grade Mesenchymal Stromal Cells Produced Under Various Good Manufacturing Practice Processes Differ in Their Immunomodulatory Properties: Standardization of Immune Quality Controls. Stem Cells and Development 2013;22:1789−801. https://doi.org/10.1089/scd.2012.0594.

[5] Chinnadurai R, Rajan D, Qayed M, Arafat D, Garcia M, Liu Y, et al. Potency Analysis of Mesenchymal Stromal Cells Using a Combinatorial Assay Matrix Approach. Cell Reports 2018;22:2504−17. https://doi.org/10.1016/j.celrep.2018.02.013.

[6] Krampera M, Cosmi L, Angeli R, Pasini A, Liotta F, Andreini A, et al. Role for interferon-gamma in the immunomodulatory activity of human bone marrow mesenchymal stem cells. Stem Cells 2006;24:386−98. https://doi.org/10.1634/stemcells.2005-0008.

[7] Lackey DE, Olefsky JM. Regulation of metabolism by the innate immune system. Nat Rev Endocrinol 2016;12:15−28. https://doi.org/10.1038/nrendo.2015.189.

[8] Michailidou Z, Gomez-Salazar M, Alexaki VI. Innate Immune Cells in the Adipose Tissue in Health and Metabolic Disease. J Innate Immun 2021: 1−27. https://doi.org/10.1159/000515117.

[9] Rocha VZ, Folco EJ, Sukhova G, Shimizu K, Gotsman I, Vernon AH, et al. Interferon-gamma, a Th1 cytokine, regulates fat inflammation: a role for adaptive immunity in obesity. Circ Res 2008;103:467−76. https://doi.org/10.1161/CIRCRESAHA.108.177105.

[10] Talukdar S, Oh DY, Bandyopadhyay G, Li D, Xu J, McNelis J, et al. Neutrophils mediate insulin resistance in mice fed a high-fat diet through secreted elastase. Nat Med 2012;18:1407−12. https://doi.org/10.1038/nm.2885.

[11] García-Rubio J, León J, Redruello-Romero A, Pavón E, Cozar A, Tamayo F, et al. Cytometric analysis of adipose tissue reveals increments of adipocyte progenitor cells after weight loss induced by bariatric surgery. Scientific Reports 2018;8:15203. https://doi.org/10.1038/s41598-018-33488-7.

[12] Ouchi N, Parker JL, Lugus JJ, Walsh K. Adipokines in inflammation and metabolic disease. Nat Rev Immunol 2011;11:85−97. https://doi.org/10.1038/nri2921.

[13] Oñate B, Vilahur G, Camino-López S, Díez-Caballero A, Ballesta-López C, Ybarra J, et al. Stem cells isolated from adipose tissue of obese patients show changes in their transcriptomic profile that indicate loss in stemcellness and increased commitment to an adipocyte-like phenotype. BMC Genomics 2013;14:625. https://doi.org/10.1186/1471-2164-14-625.

[14] Eljaafari A, Robert M, Chehimi M, Chanon S, Durand C, Vial G, et al. Adipose Tissue-Derived Stem Cells From Obese Subjects Contribute to Inflammation and Reduced Insulin Response in Adipocytes Through Differential Regulation of the Th1/Th17 Balance and Monocyte Activation. Diabetes 2015;64:2477−88. https://doi.org/10.2337/db15-0162.

[15] Serena C, Keiran N, Ceperuelo-Mallafre V, Ejarque M, Fradera R, Roche K, et al. Obesity and Type 2 Diabetes Alters the Immune Properties of Human Adipose Derived Stem Cells. Stem Cells 2016;34:2559−73. https://doi.org/10.1002/stem.2429.

[16] Strong AL, Bowles AC, Wise RM, Morand JP, Dutreil MF, Gimble JM, et al. Human Adipose Stromal/Stem Cells from Obese Donors Show Reduced Efficacy in Halting Disease Progression in the Experimental Autoimmune Encephalomyelitis Model of Multiple Sclerosis. Stem Cells 2016;34:614−26. https://doi.org/10.1002/stem.2272.

[17] Poggi M, Engel D, Christ A, Beckers L, Wijnands E, Boon L, et al. CD40L deficiency ameliorates adipose tissue inflammation and metabolic manifestations of obesity in mice. Arterioscler Thromb Vasc Biol 2011;31:2251−60. https://doi.org/10.1161/ATVBAHA.111.231357.

[18] Unek IT, Bayraktar F, Solmaz D, Ellidokuz H, Sisman AR, Yuksel F, et al. The levels of soluble CD40 ligand and C-reactive protein in normal weight, overweight and obese people. Clin Med Res 2010;8:89–95. https://doi.org/10.3121/cmr.2010.889.

[19] Denis GV, Sebastiani P, Andrieu G, Tran AH, Strissel KJ, Lombardi FL, et al. Relationships Among Obesity, Type 2 Diabetes, and Plasma Cytokines in African American Women. Obesity (Silver Spring) 2017;25:1916–20. https://doi.org/10.1002/oby.21943.

[20] Poggi M, Jager J, Paulmyer-Lacroix O, Peiretti F, Gremeaux T, Verdier M, et al. The inflammatory receptor CD40 is expressed on human adipocytes: contribution to crosstalk between lymphocytes and adipocytes. Diabetologia 2009;52:1152–63. https://doi.org/10.1007/s00125-009-1267-1.

[21] Delorme B, Ringe J, Gallay N, Le Vern Y, Kerboeuf D, Jorgensen C, et al. Specific plasma membrane protein phenotype of culture-amplified and native human bone marrow mesenchymal stem cells. Blood 2008;111:2631–5. https://doi.org/10.1182/blood-2007-07-099622.

[22] Grégoire M, Guilloton F, Pangault C, Mourcin F, Sok P, Latour M, et al. Neutrophils trigger a NF-κB dependent polarization of tumor-supportive stromal cells in germinal center B-cell lymphomas. Oncotarget 2015;6:16471–87.

[23] Luo Y, Liu M. Adiponectin: a versatile player of innate immunity. J Mol Cell Biol 2016;8:120–8. https://doi.org/10.1093/jmcb/mjw012.

[24] Hildreth AD, Ma F, Wong YY, Sun R, Pellegrini M, O'Sullivan TE. Single-cell sequencing of human white adipose tissue identifies new cell states in health and obesity. Nat Immunol 2021;22:639–53. https://doi.org/10.1038/s41590-021-00922-4.

[25] Ren G, Zhang L, Zhao X, Xu G, Zhang Y, Roberts AI, et al. Mesenchymal Stem Cell-Mediated Immunosuppression Occurs via Concerted Action of Chemokines and Nitric Oxide. Cell Stem Cell 2008;2:141–50. https://doi.org/10.1016/j.stem.2007.11.014.

[26] Raffaghello L, Bianchi G, Bertolotto M, Montecucco F, Busca A, Dallegri F, et al. Human mesenchymal stem cells inhibit neutrophil apoptosis: a model for neutrophil preservation in the bone marrow niche. Stem Cells 2008;26:151–62. https://doi.org/10.1634/stemcells.2007-0416.

[27] Hayden MS, Ghosh S. Regulation of NF-κB by TNF family cytokines. Semin Immunol 2014;26:253–66. https://doi.org/10.1016/j.smim.2014.05.004.

[28] Wilfong EM, Croze R, Fang X, Schwede M, Niemi E, López GY, et al. Proinflammatory cytokines and ARDS pulmonary edema fluid induce CD40 on human mesenchymal stromal cells—A potential mechanism for immune modulation. PLoS ONE 2020;15:e0240319. https://doi.org/10.1371/journal.pone.0240319.

[29] Nakayama Y, Brinkman CC, Bromberg JS. Murine fibroblastic reticular cells from lymph node interact with CD4+ T cells through CD40-CD40L. Transplantation 2015;99:1561–7. https://doi.org/10.1097/TP.0000000000000710.

[30] Franco G, Guarnotta C, Frossi B, Piccaluga PP, Boveri E, Gulino A, et al. Bone marrow stroma CD40 expression correlates with inflammatory mast cell infiltration and disease progression in splenic marginal zone lymphoma. Blood 2014;123:1836–49. https://doi.org/10.1182/blood-2013-04-497271.

[31] Magri G, Miyajima M, Bascones S, Mortha A, Puga I, Cassis L, et al. Innate lymphoid cells integrate stromal and immunological signals to enhance antibody production by splenic marginal zone B cells. Nat Immunol 2014;15:354–64. https://doi.org/10.1038/ni.2830.

[32] Meinderts SM, Baker G, van Wijk S, Beuger BM, Geissler J, Jansen MH, et al. Neutrophils acquire antigen-presenting cell features after phagocytosis of IgG-opsonized erythrocytes. Blood Advances 2019;3:1761–73. https://doi.org/10.1182/bloodadvances.2018028753.

[33] Jiang D, Muschhammer J, Qi Y, Kügler A, de Vries JC, Saffarzadeh M, et al. Suppression of Neutrophil-Mediated Tissue Damage-A Novel Skill of Mesenchymal Stem Cells. Stem Cells 2016;34:2393–406. https://doi.org/10.1002/stem.2417.

[34] Pedrazza L, Cunha AA, Luft C, Nunes NK, Schimitz F, Gassen RB, et al. Mesenchymal stem cells improves survival in LPS-induced acute lung injury acting through inhibition of NETs formation. J Cell Physiol 2017;232:3552–64. https://doi.org/10.1002/jcp.25816.

[35] Magaña-Guerrero FS, Domínguez-López A, Martínez-Aboytes P, Buentello-Volante B, Garfias Y. Human Amniotic Membrane Mesenchymal Stem Cells inhibit Neutrophil Extracellular Traps through TSG-6. Scientific Reports 2017;7. https://doi.org/10.1038/s41598-017-10962-2.

[36] Shang Q, Chu Y, Li Y, Han Y, Yu D, Liu R, et al. Adipose-derived mesenchymal stromal cells promote corneal wound healing by accelerating the clearance of neutrophils in cornea. Cell Death & Disease 2020;11:707. https://doi.org/10.1038/s41419-020-02914-y.

[37] Hackel A, Aksamit A, Bruderek K, Lang S, Brandau S. TNF-α and IL-1β sensitize human MSC for IFN-γ signaling and enhance neutrophil recruitment. European Journal of Immunology 2021;51:319–30. https://doi.org/10.1002/eji.201948336.

[38] Bénézech C, Mader E, Desanti G, Khan M, Nakamura K, White A, et al. Lymphotoxin-β receptor signaling through NF-κB2-RelB pathway reprograms adipocyte precursors as lymph node stromal cells. Immunity 2012;37:721–34. https://doi.org/10.1016/j.immuni.2012.06.010.

[39] Fekete N, Gadelorge M, Fürst D, Maurer C, Dausend J, Fleury-Cappellesso S, et al. Platelet lysate from whole blood-derived pooled platelet concentrates and apheresis-derived platelet concentrates for the isolation and expansion of human bone marrow mesenchymal stromal cells: production process, content and identification of active components. Cytotherapy 2012;14:540–54. https://doi.org/10.3109/14653249.2012.655420.